Arabidopsis SHORT HYPOCOTYL UNDER BLUE1 Contains SPX and EXS Domains and Acts in Cryptochrome Signaling [W]

Xiaojun Kang and Min Ni[1]

Department of Plant Biology, University of Minnesota, St. Paul, Minnesota 55108

Photomorphogenesis is regulated by red/far-red light–absorbing phytochromes and blue/UV-A light–absorbing crypto-chromes. We isolated an *Arabidopsis thaliana* blue light mutant, *short hypocotyl under blue1* (*shb1*), a knockout allele. However, *shb1-D*, a dominant allele, exhibited a long-hypocotyl phenotype under red, far-red, and blue light. The phenotype conferred by *shb1-D* was caused by overaccumulation of *SHB1* transcript and recapitulated by overexpression of *SHB1* in *Arabidopsis*. Therefore, SHB1 acts in cryptochrome signaling but overexpression may expand its signaling activity to red and far-red light. Consistent with this, overexpression of *SHB1* enhanced the expression of *PHYTOCHROME-INTERACTING FACTOR4* (*PIF4*) under red light. PIF4 appears to specifically mediate SHB1 regulation of hypocotyl elongation and *CHLOROPHYLL a/b BINDING PROTEIN3* or *CHALCONE SYNTHASE* expression under red light. Overexpression of *SHB1* also promoted proteasome-mediated degradation of phytochrome A and hypocotyl elongation under far-red light. Under blue light, *shb1* suppressed *LONG HYPOCOTYL IN FAR-RED LIGHT1* (*HFR1*) expression and showed several deetiolation phenotypes similar to *hfr1-201*. However, the hypocotyl and cotyledon-opening phenotypes of *shb1* were opposite to those of *hfr1-201*, and HFR1 acts downstream of SHB1. *SHB1* encodes a nuclear and cytosolic protein that has motifs homologous with SYG1 protein family members. Therefore, our studies reveal a signaling step in regulating cryptochrome- and possibly phytochrome-mediated light responses.

INTRODUCTION

Plants have evolved red and far-red light–absorbing phyto-chromes and UV-A/blue light–absorbing cryptochromes and phototropins (Neff et al., 2000; Huq and Quail, 2005). Among the photoreceptors, phytochromes and cryptochromes regulate seedling deetiolation responses, including the inhibition of hy-pocotyl elongation, the opening of hypocotyl hooks, the opening and expansion of cotyledons, and the development of chloro-plasts. In *Arabidopsis thaliana*, the phytochrome gene family has five members, *PHYA* through *PHYE* (Huq and Quail, 2005). phyA is the photoreceptor for far-red light–mediated deetiolation re-sponses, and phyB is the major photoreceptor for red light–mediated deetiolation responses. Purified oat (*Avena sativa*) phyA preparations have been shown to autophosphorylate and to phosphorylate PHYTOCHROME SUBSTRATE1 (PKS1), cryp-tochrome1 (cry1), and auxin/indole-3-acetic acid proteins in vitro (Ahmad et al., 1998; Yeh and Lagarias, 1998; Fankhauser et al., 1999; Colón-Carmona et al., 2000). phyA and phyB also trans-locate to the nucleus in a light-dependent manner and interact with PHYTOCHROME-INTERACTING FACTOR1 (PIF1), PIF3, and PIF4, PKS1, NUCLEOSIDE DIPHOSPHATE KINASE2, ARABI-

DOPSIS RESPONSE REGULATOR4, EARLY FLOWERING3 (ELF3), PHYTOCHROME-ASSOCIATED PROTEIN PHOSPHA-TASE, and PHYTOCHROME-SPECIFIC TYPE 5 PHOSPHATASE in vitro (Ni et al., 1998, 1999; Choi et al., 1999; Fankhauser et al., 1999; Kircher et al., 1999; Liu et al., 2001; Sweere et al., 2001; Kim et al., 2002; Huq and Quail, 2005; Ryu et al., 2005).

Mutations in *CRY1* impair seedling deetiolation responses under blue/UV-A light (Yang et al., 2000; Cashmore, 2003). *CRY1* encodes a flavoprotein with sequence similarity to photolyases but lacks photolyase activity and has a C-terminal extension not found in the photolyases. Dark-grown *Arabidopsis* seedlings carrying the C-terminal domains of either cry1 or cry2 show phenotypes that are normally associated with light-grown seed-lings and are often observed for *constitutive photomorphogenic1* (*cop1*) (Yang et al., 2000). The signaling activity of cry1, therefore, probably involves a direct interaction of its C terminus with COP1, a negative regulator of photomorphogenesis (Wang et al., 2001; Yang et al., 2001). cry2 is involved in the control of pho-toperiodic flowering in addition to its role in regulating seedling deetiolation responses (Guo et al., 1998; Lin et al., 1998). cry1, when fused with GREEN FLUORESCENT PROTEIN (GFP), was localized in the nucleus in a transient expression system or in dark-grown transgenic *Arabidopsis* seedlings, but it was primar-ily in the cytoplasm under continuous white light conditions (Guo et al., 1999; Yang et al., 2000). Although light induces a trans-location of cry1 to the cytoplasm, cry1 signaling may involve both nuclear and cytosolic events, and early cry1 signaling may still operate in the nucleus. By contrast, cry2 was localized predominantly to the nucleus under dark or light conditions (Guo et al., 1999; Kleiner et al., 1999; Yang et al., 2000). Both cry1 and cry2 undergo a blue light–dependent phosphorylation, and the

phosphorylation status may be closely associated with their regulatory functions (Shalitin et al., 2002, 2003). cry1, when expressed and purified from insect cells, is also phosphorylated in a blue light–dependent manner, consistent with an autophosphorylation function of cry1 (Bouly et al., 2003). cry2 protein is unstable, and this instability may be mediated by its interaction with COP1 (Wang et al., 2001).

Genetic screens have identified many far-red light signaling mutants, and nine of the genes affected in these mutants have been identified (for review, see Huq and Quail, 2005). Genetic screens have also identified mutants with defects in red light responses, such as *gigantean* (*gi*), *pif4*, *elf3*, and *sensitivity to red light-reduced1* (*srr1*), or in both red and far-red light responses, such as *phytochrome signaling early flowering1*, *pseudoresponse regulator7*, and *phytochrome signaling2* (Huq and Quail, 2005). Many light signaling components are nuclear proteins, whereas others, such as FAR-RED INSENSITIVE219 (FIN219) and PHYTOCHROME A SIGNAL TRANSDUCTION1 (PAT1), are cytosolic proteins. FAR-RED ELONGATED HYPOCOTYL1 (FHY1) and SRR1 exist in both the nucleus and the cytoplasm (Staiger et al., 2003; Huq and Quail, 2005). A blue light–specific component, PHOSPHATASE7 (PP7), was isolated recently, and *PP7* encodes a Ser/Thr protein phosphatase (Møller et al., 2003). SHORT UNDER BLUE1, a cytoplasmic calcium binding protein, has a major function in cryptochrome signaling but also modulates phyA-mediated far-red light responses (Guo et al., 2001). HFR1, a basic helix-loop-helix protein identified previously for its involvement in far-red light signaling, also plays a role in regulating several blue light–mediated responses (Duek and Fankhauser, 2003). In addition, HYPERSENSITIVE TO RED AND BLUE1 (HRB1), PIF4, and OBF BINDING PROTEIN3 have been shown recently to act in both red and blue signaling (Kang et al., 2005; Ward et al., 2005).

Mutants in a different class, *cop/deetiolated/fusca*, exhibit a light-grown phenotype even when grown in darkness and identify a total of 11 loci. Many of the proteins encoded are involved in control of the stability of a few key light signaling components, such as LONG HYPOCOTYL IN THE LIGHT5 (HY5), LONG AFTER FAR-RED LIGHT1 (LAF1), and HFR1 (Osterlund et al., 2000; Seo et al., 2003; Jang et al., 2005; Yang et al., 2005). Early biochemical studies using microinjection and pharmacological techniques have also suggested the involvement of cyclic GMP, G-proteins, protein phosphatase, and calcium/calmodulin in phytochrome signaling (Neuhaus et al., 1997; Huq and Quail, 2005). Recent genetic studies have further suggested the involvement of G-protein in light signaling (Okamoto et al., 2001; Jones et al., 2003).

We have isolated a new long-hypocotyl mutant, *shb1-D*, under red, far-red, and blue light conditions. The long-hypocotyl phenotype of *shb1-D* is caused by the overexpression of its wild-type gene. By contrast, *shb1*, a knockout allele, exhibits hypocotyl and cotyledon phenotypes mostly under blue light. SHB1 is localized in the nucleus and the cytoplasm and regulates various light responses either positively or negatively. The transcript of *SHB1* is extremely low, and the level of SHB1 protein may be limiting for red and far-red light signaling, or the lack of hypocotyl and cotyledon phenotypes in *shb1* under red or far-red light may be attributable to a redundant function of SHB1 homologues. Consistent with this possibility, overexpression of *SHB1*

activated the expression of *PIF4* and PIF4-mediated red light signaling, and also promoted phyA degradation and hypocotyl elongation under far-red light. Moreover, SHB1 signaling under blue light may involve HFR1, and the *shb1* mutation indeed suppressed the expression of *HFR1* under blue light. Double mutant analysis suggested that *hfr1-201* is epistatic to *shb1* in hypocotyl growth regulation and cotyledon opening responses under blue light. Interestingly, blue and red light signaling of SHB1 appears to involve two basic helix-loop-helix proteins, PIF4 and HFR1, important for both cryptochrome and phytochrome signaling.

RESULTS

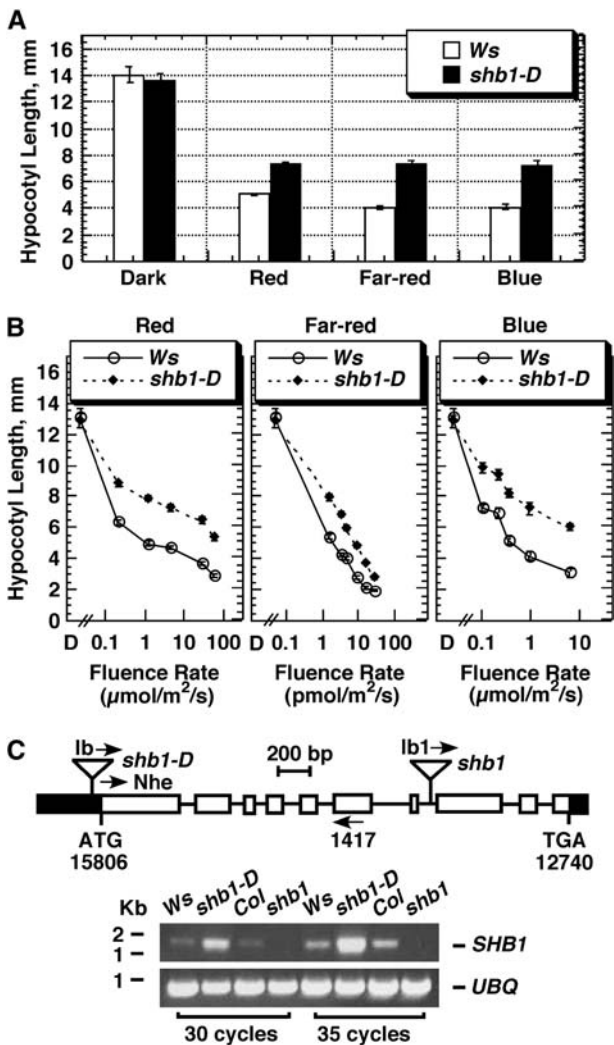### *shb1-D* Has a Long-Hypocotyl Phenotype under Red, Far-Red, and Blue Light

We screened a collection of 40,000 lines containing T-DNA insertions (ABRC) for mutants with either a short- or long-hypocotyl phenotype under red light. One mutant identified, *shb1-D* (for *short hypocotyl under blue1 Dominant*), showed a long-hypocotyl phenotype under red and far-red light (Figure 1A). Subsequently, *shb1-D* was also identified to have a long-hypocotyl phenotype under blue light. The long-hypocotyl phenotype of *shb1-D* appeared persistent over a broad range of red and blue light intensities (Figure 1B, left and right). By contrast, *shb1-D* exhibited a stronger hypocotyl phenotype under relatively weak or intermediate intensities of far-red light, ranging from 1 to 7 pmol·m^{-2}·s^{-1} (Figure 1B, middle).

Molecular Cloning of *SHB1*

By backcrossing *shb1-D* to Wassilewskija (Ws), we found that *shb1-D* has a T-DNA insertion at a single genetic locus and a dominant phenotype, and the T-DNA insertion is tightly linked to the mutation. We cloned the mutated gene by walking to the flanking plant genomic sequence using a GenomeWalker kit (see Methods). In *shb1-D*, the T-DNA left border is inserted at transformation-competent BAC clone T30C3 sequence 15935, 129 bp upstream of the start codon of a predicted gene, At4g25350, on chromosome 4 (Figure 1C). The putative gene is composed of 10 exons and 9 introns. An additional database search identified a second T-DNA insertional allele, *shb1*, from the SALK T-DNA insertion collection. The T-DNA left border is inserted at transformation-competent BAC clone T30C3 sequence 13588, 8 bp from the beginning of the eighth exon of the putative gene (Figure 1C). Among six plants propagated from the original SALK seeds, four plants were found to be wild type and two plants were found to be heterozygous based on both PCR genotyping and kanamycin resistance. The two heterozygous lines showed a 3:1 segregation ratio of their kanamycin resistance, suggesting a single T-DNA insertion in *shb1*. Homozygous lines were subsequently identified from the heterozygous parents. Both T-DNA insertions in *shb1-D* and *shb1* were verified using PCR techniques (see Supplemental Figure 1 online).

SHB1 Is Overexpressed in *shb1-D* but Is Knocked Out in *shb1*

SHB1 message was extremely low in total RNA preparations from the Ws wild type, and we failed to detect it through RNA gel

Figure 1. *shb1-D* Shows a Long-Hypocotyl Phenotype under Red, Far-Red, and Blue Light.

(A) Hypocotyl growth responses of Ws and *shb1-D* to continuous red light (15 μmol·m^{-2}·s^{-1}), far-red light (10 pmol·m^{-2}·s^{-1}), or blue light (3 μmol·m^{-2}·s^{-1}) for 4 d. Data are presented as means ± SE.

(B) Hypocotyl fluence responses of Ws and *shb1-D* to continuous red, far-red, and blue light for 4 d. Data are presented as means ± SE.

(C) *SHB1* is upregulated in *shb1-D* but is knocked out in *shb1*. Top, the *SHB1* gene structure shows sequence coordination from BAC clone T30C3. Black boxes represent the 5′ and 3′ untranslated regions. White boxes indicate exons, and lines indicate introns. Bottom, RT-PCR analysis of *SHB1* expression using 0.5 μg of total RNA prepared from Ws, *shb1-D*, Col, and *shb1*. RT-PCR analysis was run for 30 and 35 cycles using the primer pair Nhe and 1417. Control RT-PCR was run for *UBQ10* under identical conditions.

blot hybridization analysis. Instead, RT-PCR analysis with the primer pair Nhe and 1417 revealed a detectable level of *SHB1* mRNA in Ws but a very high level of *SHB1* mRNA in *shb1-D* (Figure 1C, bottom). To exclude a possible difference in the quality of RNA preparations, we performed a control RT-PCR analysis for *UBIQUITIN10* (*UBQ10*) and detected fairly constant

levels of *UBQ10* messages in Ws and *shb1-D* (Figure 1C, bottom). However, the reason for the increased level of *SHB1* mRNA in *shb1-D* remains unknown. It is possible that an enhancer element carried on the T-DNA insertion may activate the transcription of *SHB1* downstream. Alternatively, the T-DNA insertion may inactivate a negative regulatory element in the *SHB1* gene promoter region. To learn the consequence of the T-DNA insertion on *SHB1* expression in *shb1*, we performed an additional RT-PCR analysis using a 5′ primer, Nhe, and a 3′ primer, 1417, positioned before the T-DNA insertion. RT-PCR analysis with this pair of primers failed to detect *SHB1* transcript in *shb1*, and the T-DNA insertion apparently resulted in a loss of *SHB1* expression in *shb1* (Figure 1C, bottom).
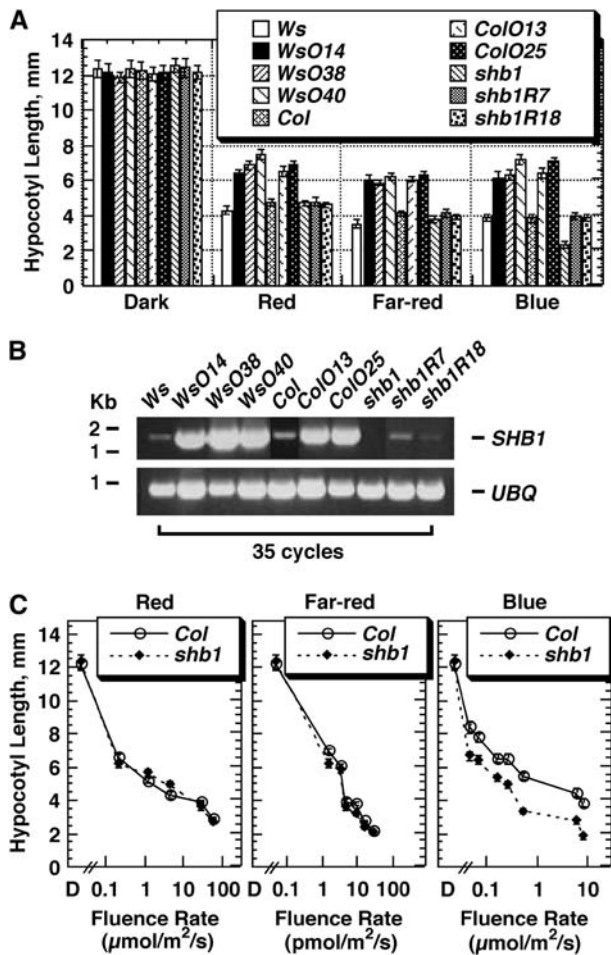
Overexpression of *SHB1* Recapitulates the Phenotype Conferred by *shb1-D*, and *shb1* Has a Short-Hypocotyl Phenotype under Blue Light

Given the gain-of-function phenotype of *shb1-D*, we performed additional experiments to verify the cause of the long-hypocotyl phenotype in *shb1-D* (Figure 2A). We generated transgenic plants that carry a single T-DNA insertion with a *SHB1* coding sequence under the control of the cauliflower mosaic virus (CaMV) 35S promoter in either the Ws or Columbia (Col) background. Several representative lines, homozygous for the transgenes in either the Ws or Col background, all exhibited a long-hypocotyl phenotype under red, far-red, and blue light (Figure 2A). RT-PCR analysis demonstrated that *SHB1* was indeed overexpressed in these transgenic lines (Figure 2B).

The original wild-type and heterozygous *shb1* individuals derived from the SALK seeds, as well as the wild-type, heterozygous, and homozygous decedents of the original heterozygous individuals, were all further tested for their hypocotyl growth responses under various light conditions. Homozygous *shb1* individuals showed a short-hypocotyl phenotype only under blue light, and the short-hypocotyl phenotype is particularly pronounced under moderate to strong blue light (Figure 2C). By contrast, heterozygous individuals showed a hypocotyl growth response much similar to wild-type individuals, indicating the recessive nature of the *shb1* mutation and the tight linkage of the T-DNA insertion to the phenotype observed. We then introduced a 4.7-kb genomic fragment, containing a 1.2-kb *SHB1* promoter sequence, the *SHB1* coding sequence, and 0.5 kb of 3′ sequence, into *shb1*. The introduced genomic fragment resulted in a wild-type level of expression of *SHB1* and fully complemented the hypocotyl phenotype of *shb1* to the wild type (Figures 2A and 2B).

Mutations in *SHB1* Alter Other Light Responses

When wild-type seedlings are grown under far-red light for several days, they have low survival success after being transferred to white light, a phenomenon known as far-red light preconditioned block of greening (Neff et al., 2000; Huq and Quail, 2005). Under such conditions, the survival rate for Col wild-type seedlings was 23%, whereas *phyA-211* had a survival rate of 99% (Figure 3A). Similar to *phyA-211*, *shb1-D* had a significantly higher survival rate (81%) than its Ws wild type (15%).

Figure 2. Overexpression of *SHB1* Recapitulates the Long-Hypocotyl Phenotype of *shb1-D*, and *shb1* Shows a Short-Hypocotyl Phenotype under Blue Light.

(A) Hypocotyl growth responses of Ws, *shb1-D*, *SHB1* overexpression lines in the Ws background (WsOE14, WsOE38, and WsOE40), Col, *SHB1* overexpression lines in the Col background (ColOE13 and ColOE25), *shb1*, and *shb1* rescue lines (*shb1-2*R7 and *shb1*R18) to continuous red, far-red, or blue light for 4 d under intensities as specified for Figure 1A. Data are presented as means ± SE.
(B) RT-PCR analysis of *SHB1* expression using 0.5 μg of total RNA isolated from white light-grown Ws, *shb1-D*, Col, *shb1*, and various *SHB1* overexpression or *shb1* rescue lines (top). Controls were performed for *UBQ10* under identical conditions (bottom).
(C) Hypocotyl fluence responses of Col and *shb1* to continuous red, far-red, or blue light for 4 d. Data are presented as means ± SE.

A *SHB1* overexpression line in the Col background, ColOE25, also had a significantly higher survival rate (78%) than its Col wild type (23%).

Six days after germination, the rate of light-induced cotyledon expansion in *shb1-D* was rather enhanced. Both *shb1* and line ColOE25 had larger cotyledons than the Ws or Col wild type under red or blue light at this early developmental stage (Figure 3B). The knockout allele, *shb1*, had much smaller cotyledons under blue light than its Col wild type at the same developmental

stage (Figure 3B). Twenty-one days after germination, *shb1* and line ColOE25 developed smaller leaves than the Ws or Col wild type under white light, resembling that of *phyB-9* (Figure 3C; data not shown). As a result, *shb1-D* looked quite different from either the wild type or *phyB-9* (Figure 3C). At the same developmental stage, *shb1-D* and line ColOE25 developed short petioles (Figure 3D). By contrast, *shb1* plants had longer petioles than did Col wild-type plants (Figure 3D).

Mutations in *SHB1* Affect Pigment Accumulation and *CHLOROPHYLL a/b BINDING PROTEIN3* or *CHALCONE SYNTHASE* Expression

Under red and blue light, 5-d-old seedlings of *shb1-D* and line ColOE25 accumulated much more chlorophylls than did Ws or Col wild-type plants (Figure 4A). *shb1-D* and line ColOE25 also accumulated more anthocyanin pigments under red, far-red, and blue light than did Ws or Col wild-type plants (Figure 4B). By contrast, *shb1* accumulated a normal amount of chlorophylls under all light conditions tested but less anthocyanin pigments under far-red and blue light (Figures 4A and 4B). Chlorophyll biosynthesis is coordinately regulated with the expression of chlorophyll *a/b* binding protein genes (McCormack and Terry, 2002), and we further examined the expression of *CHLORO-PHYLL a/b BINDING PROTEIN3* (*CAB3*), one member of this gene family, under red, far-red, and blue light.

The level of *CAB3* expression in Ws or Col plants is very low in darkness, but it is strongly induced by red, far-red, and blue light. The light-induced expression of *CAB3* was enhanced threefold over that of Ws by *shb1* under red light, but it remained the same as in the Ws wild type under far-red and blue light (Figure 4C). By contrast, *shb1* did not affect the light-induced expression of *CAB3* under all light conditions tested (Figure 4D). We also examined the light-induced expression of *CHALCONE SYN-THASE* (*CHS*), a gene that encodes an enzyme involved in flavonoid and anthocyanin biosynthesis. The level of *CHS* expression is very low in darkness, but it was induced by red, far-red, and blue light in either Ws or Col wild-type plants. *shb1-D* caused a further accumulation of *CHS* transcripts, 3.0-, 2.4-, and 2.0-fold, compared with that in Ws under red, far-red, and blue light, respectively (Figure 4C). By contrast, *shb1* attenuated the light-induced accumulation of *CHS* transcripts by 2.5-fold under far-red and blue light (Figure 4D). Because *CHS* encodes the first committed enzyme in anthocyanin biosynthesis, the amount of anthocyanin accumulation may be influenced by the overexpression or underexpression of *CHS* in *shb1-D* or *shb1*.

cry Mutants Are Epistatic to *shb1*

To learn the roles of SHB1 in light signaling in relation to photoreceptors, we generated double mutants of *shb1-D* with *phyA*, *phyB*, *cry1*, or *cry2*, and of *shb1* with *cry1* or *cry2*. Either *shb1-D phyB-9* or *shb1-D phyA-211* double mutant showed the severe hypocotyl phenotypes of the *phyB-9* or *phyA-211* single mutant, respectively, under red and far-red light (Figure 5). Under blue light, *shb1-D* showed a moderate hypocotyl phenotype very similar to that of *phyA-211* or *cry2*, and *shb1-D phyA-211* or *shb1-D cry2* exhibited a hypocotyl phenotype indistinguishable
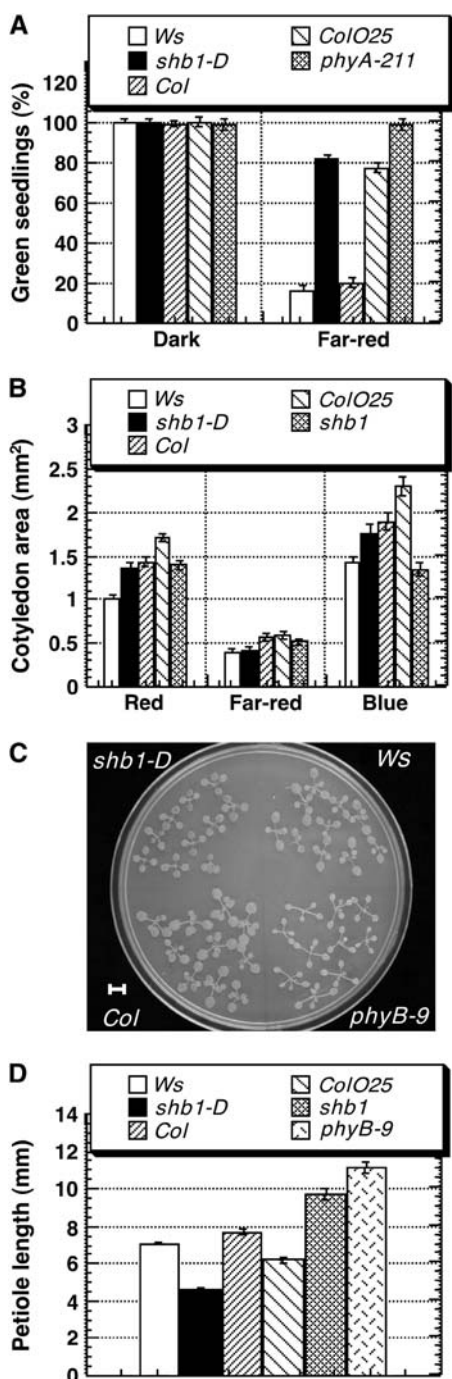
Figure 3. Mutations in *SHB1* Alter Other Light Responses.

(A) Percentage of green seedlings of Ws, *shb1-D*, Col, *SHB1* over-expression line 25 in the Col background (ColO25), and *phyA-211*, grown either in darkness or under far-red light (1 μmol·m^{-2}·s^{-1}) for 4 d, and then transferred to white light for an additional 6 d. Data are presented as means ± SE.

(B) Cotyledon size, measured 6 d after germination, for Ws, *shb1-D*, Col, line ColO25, and *shb1* seedlings grown under continuous red, far-red, or blue light at intensities as indicated for Figure 1A. Data are presented as means ± SE.

from either of their mutant parents (Figure 6A; see Supplemental Figure 2 online). *cry1* had the most severe hypocotyl phenotype under blue light, and *shb1-D cry1* showed the severe hypocotyl phenotype of *cry1* (Figure 6A). Thus, *shb1-D* does not suppress or enhance the *phy* and *cry* hypocotyl phenotypes.

We also generated double mutants of *shb1* with *cry1* or *cry2*. Under blue light, *shb1* has a shorter hypocotyl phenotype, whereas *cry1* or *cry2* has a longer hypocotyl phenotype. Either *shb1 cry1* or *shb1 cry2* double mutant showed a hypocotyl phenotype similar to that of *cry1* or *cry2* (Figure 6B). This epistasis may indicate that the expression of the phenotype conferred by *shb1* requires either functional cry1 or cry2. We noticed that the hypocotyl length of either the wild type or *cry2* under 0.6 μmol·m^{-2}·s^{-1} blue light was shorter than that reported under equivalent light intensity (Lin et al., 1998). The difference between our results and those previous results may be attributed to the different light sources used.

SHB1 Contains an SPX Domain and an EXS Domain Found in the SYG1 Protein Family

SHB1 contains an N-terminal SPX domain and a C-terminal EXS domain found in yeast SYG1 protein (gi 731805) and mouse XENOTROPIC AND POLYTROPIC MURINE LEUKEMIA VI-RUSES RECEPTOR1 (XPR1) protein (gi 6093320) (Figure 7A; see Supplemental Figure 3 online). The SPX domain (pfam03105 family) is named after SYG1, PHOSPHATE TRANSPORTER81 or PHO81, and XPR1, whereas the EXS domain (pfam03124 family) is named after ER RETENTION-DEFECTIVE1 or ERD1, XPR1, and SYG1. The SPX domain can also be found in several predicted proteins of uncertain function from *Arabidopsis* (gi 3548805 and gi 3548806), *Drosophila melanogaster* (gi 22832470, gi 22946878, and gi 7290442), *Saccharomyces cerevisiae* (gi 731951), and *Schizosaccharomyces pombe* (gi 5832411). SHB1 is relatively closer to one SYG1 or XPR1 homologue from yeast (gi 731951) and two SYG1 or XPR1 homologues from *Arabidopsis* (gi 3548805 and gi 3548806) than to other SYG1 or XPR1 homologues from yeast, fission yeast, *Neurospora*, worm, fly, mouse, and human (see Supplemental Figures 3 and 4 online). The consensus sequences derived from all SYG1 homologues, and the alignment of SHB1 with SYG1 protein from yeast, are presented for both SPX and EXS domains (see Supplemental Figure 5 online).

The EXS region of similarity contains several predicted trans-membrane helices. For example, yeast SYG1 is predicted to contain eight membrane-spanning motifs, and three motifs are predicted in the EXS domain. Another five motifs are located between the SPX domain and the EXS domain. As demonstrated by cell fractionation techniques, yeast SYG1 is localized to a fraction enriched in plasma membrane (Spain et al., 1995).

(C) Ws, *shb1-D*, Col, and *phyB-9* plants, grown under continuous white light (30 μmol·m^{-2}·s^{-1}) for 21 d after germination, and transferred to an agar plate for photography. Bar = 4 mm.

(D) Petiole length, measured 21 d after germination, for Ws, *shb1-D*, Col, line ColO25, *shb1*, and *phyB-9* plants grown under continuous white light (30 μmol·m^{-2}·s^{-1}). Data are presented as means ± SE.
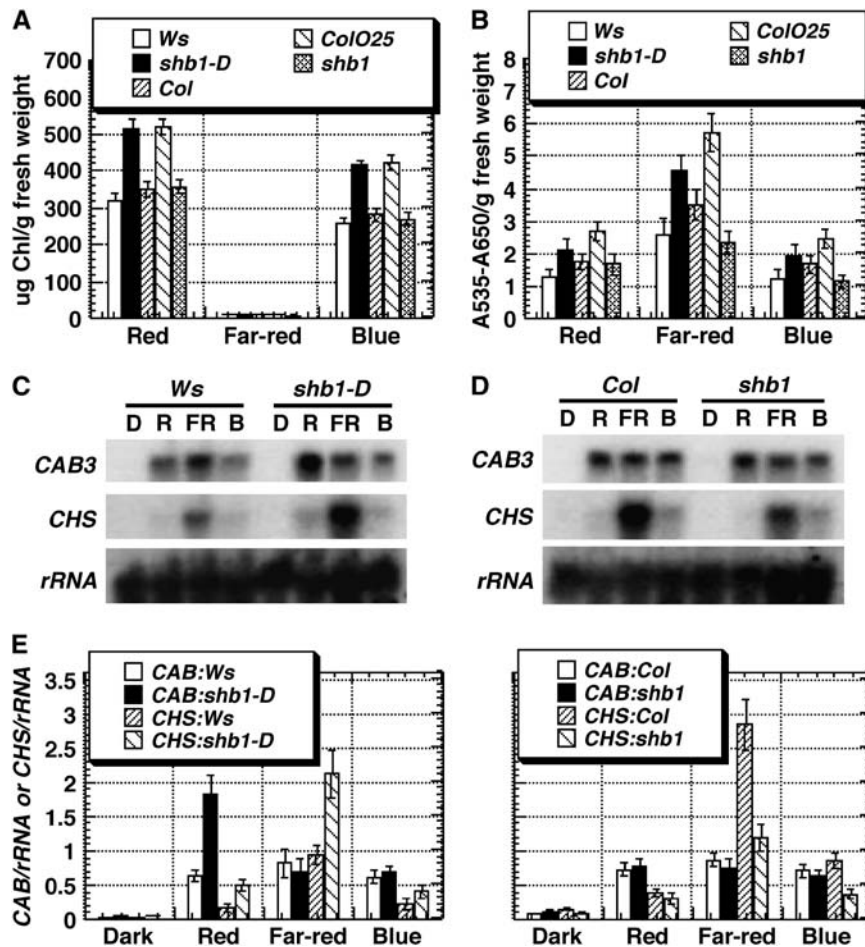
Figure 4. Mutations in *SHB1* Alter Pigment Accumulation and *CAB3* or *CHS* Expression.

(A) and **(B)** Chlorophyll **(A)** and anthocyanin **(B)** content of 5-d-old Ws, *shb1-D*, Col, line ColO25, and *shb1* seedlings grown under red, far-red, or blue light at intensities as indicated for Figure 1A. Data are presented as means of three independent biological replicates ± SE.

(C) and **(D)** RNA gel blot hybridization analysis of *CAB3* and *CHS* expression in Ws and *shb1-D* **(C)** or in Col and *shb1* **(D)**. Total RNA was isolated from 5-d-old dark-grown seedlings that received no light treatment (D) or were treated for 4 h with red (R), far-red (FR), or blue (B) light under intensities as specified for Figure 1A.

(E) Normalization of *CAB3* and *CHS* mRNA levels to 18 *rRNA* signals. The hybridization signals were detected with a PhosphorImager (Molecular Dynamics) screen and quantified using the ImageQuant program. Data are presented as means ± SE from three independent experiments.

Examination of the SHB1 sequence with the PSORT program also identified six weakly predicted integral membrane motifs (certainty, 0.6) located in amino acid sequences 347 to 363, 429 to 445, 465 to 481, 492 to 508, 559 to 575, and 665 to 681. The fifth and sixth motifs fall within the predicted EXS domain.

SHB1 Is Localized in the Nucleus and the Cytoplasm

Recently, genomic scale profiling has identified SHB1 (gi 7487574 or At4g25350) as PHO1 homologue 4, or H4, a member of the PHO1 family of putative phosphate transporters (Wang et al., 2004). The PHO1 family comprises 11 members, and PHO1 is involved in the loading of inorganic phosphate into the xylem of roots (Hamburger et al., 2002). Phylogenetic analysis also showed that SHB1 (gi 7487574) is more closely related to two

Arabidopsis PHO1 homologues (gi 3548805 or At2g03250 and gi 3548806 or At2g03249) and a yeast protein, PHO84 (gi 731951) (see Supplemental Figure 3A online). PHO84 is described as a member of the PHO family involved in low-affinity inorganic phosphate transport and potentially phosphate sensing (Wykoff and O'Shea, 2001). Thus, the homology of SHB1 with the *Arabidopsis* and yeast proteins may suggest a potential role of SHB1 in phosphate homeostasis.

To investigate the subcellular localization of SHB1, we constructed a *SHB1*:β-D-glucuronidase (*GUS*) fusion in pBI221 and conducted a transient transfection assay using onion (*Allium cepa*) epidermal peels. In darkness, SHB1:GUS was clearly localized in the nucleus and the cytosol in these onion epidermal cells (Figure 7B). Treatment with white, red, far-red, or blue light for 4 and 8 h did not alter the pattern of SHB1:GUS subcellular
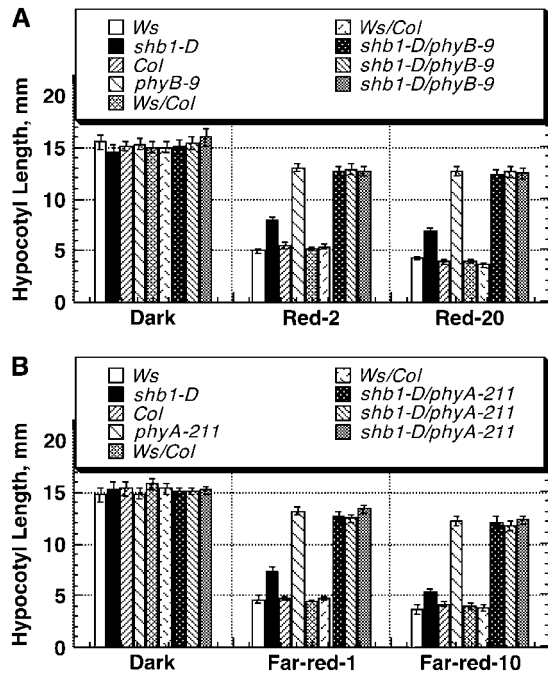
Figure 5. Double Mutant Analysis of *shb1-D* with *phyB-9* or *phyA-211* under Red or Far-Red Light.

(A) Hypocotyl growth responses of Ws, *shb1-D*, Col, *phyB-9*, Ws/Col lines, and multiple *shb1-D phyB-9* lines to 2 or 20 μmol·m^{-2}·s^{-1} red light (Red-2 or Red-20) for 4 d. Data are presented as means ± SE.

(B) Hypocotyl growth responses of Ws, *shb1-D*, Col, *phyA-211*, Ws/Col lines, and multiple *shb1-D phyA-211* lines to 1 or 10 pmol·m^{-2}·s^{-1} far-red light (Far-red-1 or Far-red-10) for 4 d. Data are presented as means ± SE.

localization (data not shown). The staining of SHB1:GUS was particular enriched in the nucleus, and the staining in the cytosol therefore may not be as strong as that of GUS alone (Figure 7B). Therefore, the nuclear and cytosolic localization of SHB1 may suggest a role of SHB1 in light signaling rather than in organic phosphate transport.

SHB1 Is Required for the Proper Expression of *PIF4* and *HFR1*

To further explore the role of SHB1 in cryptochrome or phytochrome signaling, we surveyed the expression of many light signaling genes identified to date in *shb1-D* or *shb1* under red, far-red, and blue light using RT-PCR techniques. The genes include *PP7*, *HRB1*, *PIF3*, *PIF4*, *ELF3*, *ELF4*, *GI*, *SRR1*, *FHY1*, *FHY3*, *HFR1*, *FAR-RED IMPAIRED RESPONSE1*, *LAF1*, *PAT1*, *SUPPRESSOR OF PHYTOCHROME-105 1*, *EMPFINDLICHER IM DUNKELROTEN LICHT1*, *FIN219*, and *HY5* (Huq and Quail, 2005). We detected changes in the expression of *PIF4* and *HFR1* in both *shb1-D* and *shb1* and subsequently verified the changes using RNA gel blot hybridization analysis (Figure 8A). The expression of *PIF4* in either the Ws or Col wild type was strongly induced by red, far-red, and blue light (Huq and Quail, 2002) (Figure 8A). Compared with the Ws or Col wild type,

overexpression of *SHB1* in *shb1-D* resulted in a further 3.2-fold increase in *PIF4* expression under red light, whereas loss of *SHB1* expression in *shb1* led to a 3.2-fold decrease in *PIF4* expression under red light (Figure 8A). By contrast, the effects of *shb1-D* or *shb1* on *PIF4* expression were not obvious under either far-red or blue light. Comparable changes in the expression of *PIF4* caused by either *shb1-D* or *shb1* under red light were also observed using real-time PCR analysis (Figure 8B, left). Consistent with RNA gel blot hybridization analysis, real-time PCR did not reveal any changes in the expression of *PIF4* in either *shb1-D* or *shb1* under far-red or blue light.

The expression of another basic helix-loop-helix gene, *HFR1*, in either the Ws or Col wild type was induced strongly by far-red light and moderately by blue light (Figure 8A) (Duek and Fankhauser, 2003). Under red light, the expression of *HFR1* was weakly induced by a 4-h red light treatment (Figure 8A). However, Duek and Fankhauser (2003) only observed a slight increase in *HFR1* message up to 2 or 4 h and a sharp reduction in HFR1 message after 4 h of red light treatment. Overexpression of *SHB1* in *shb1-D* caused further 2.6- and 2.5-fold increases in the expression of *HFR1* under red and blue light, respectively, compared with the Ws wild type (Figure 8B). By contrast, lack
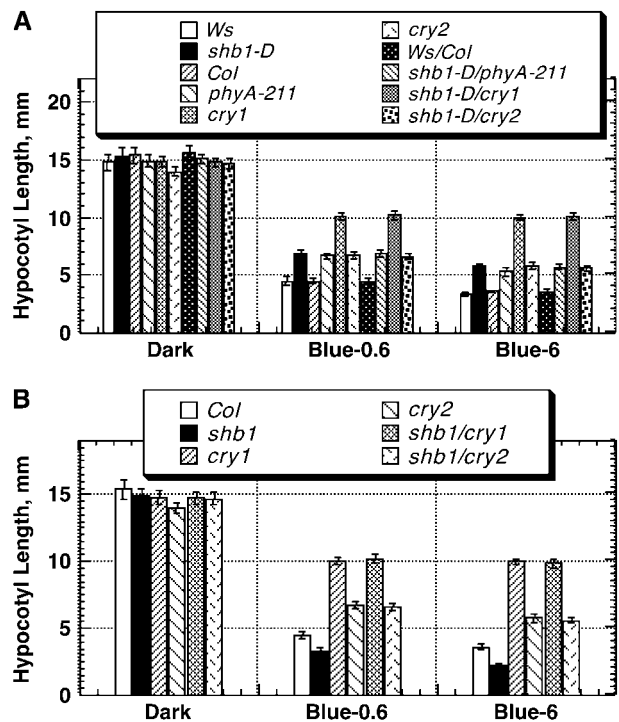
Figure 6. Double Mutant Analysis of *shb1-D* with *phyA-211* and *cry* Mutants and of *shb1* with *cry* Mutants under Blue Light.

(A) Hypocotyl growth responses of Ws, *shb1-D*, Col, *phyA-211*, *cry1*, *cry2*, Ws/Col, *shb1-D phyA-211*, *shb1-D cry1*, and *shb1-D cry2* to 0.6 or 6 μmol·m^{-2}·s^{-1} blue light (Blue-0.6 or Blue-6) for 4 d. Data are presented as means ± SE.

(B) Hypocotyl growth responses of Col, *shb1*, *cry1*, *cry2*, *shb1 cry1*, and *shb1 cry2* to 0.6 or 6 μmol·m^{-2}·s^{-1} blue light (Blue-0.6 or Blue-6) for 4 d. Data are presented as means ± SE.
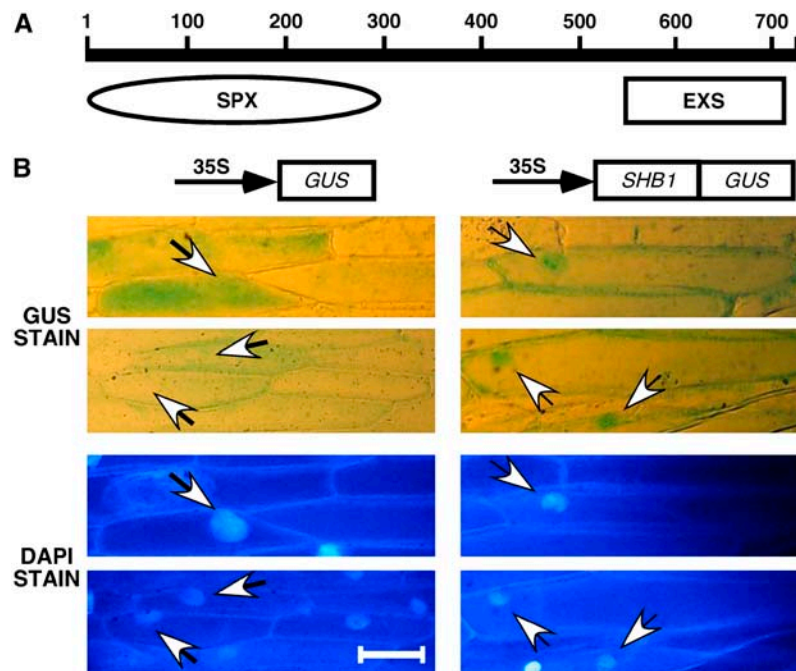
Figure 7. SHB1 Is Localized to the Nucleus and the Cytosol.

(A) Diagram shows the N-terminal SPX domain and the C-terminal EXS domain in the SHB1 protein.
(B) Subcellular localization of GUS (left) or the SHB1:GUS fusion protein (right) in onion epidermal cells (arrows, top panels), and 4′,6-diamidino-2-phenylindole (DAPI) stain for the location of the nuclei (arrows, bottom panels). The images were taken for onion epidermal layers incubated in darkness. Bar = 100 μm.

of *SHB1* expression in *shb1* resulted in 2.4- and 1.7-fold decreases in the expression of *HFR1* under red and blue light, respectively (Figure 8B). No changes in *HFR1* expression were observed under far-red light in either *shb1-D* or *shb1*. Because some of the changes observed were less than twofold, we performed real-time PCR analysis to further verify the RNA gel blot analysis data. The increases caused by *shb1-D* on *HFR1* expression under red and blue light were 3.1- and 2.7-fold, respectively, greater than that in the Ws wild type, whereas *shb1* caused 2.6- and 2.7-fold decreases in *HFR1* expression under red and blue light, respectively, compared with the Ws wild type (Figure 8C). Real-time PCR analysis revealed slightly larger decreases in the expression of *HFR1* by *shb1* than those observed through RNA gel blot hybridization analysis (Figures 8B and 8C).

PIF4 Specifically Mediates SHB1 Regulation of Hypocotyl Elongation and *CAB3* or *CHS* Expression under Red Light

Because the expression of *PIF4* was affected in *shb1-D* or *shb1* under red light, we further examined the genetic interactions that control hypocotyl elongation and light-regulated gene expression responses. *shb1-D* has a longer hypocotyl and *pif4* has a shorter hypocotyl under both red and blue light compared with the Ws wild type, whereas the *shb1-D pif4* double mutant showed a *pif4*-like hypocotyl phenotype under red light but an *shb1-D*–like hypocotyl phenotype under blue light (Figure 9A). Apparently, the expression of the *shb1-D* hypocotyl phenotype

under blue light was independent of the *pif4* mutation. Similar genetic interactions were also observed for their light-induced gene expression responses. Under red light, *shb1-D* enhanced but *pif4* reduced the expression of *CAB3* and *CHS*, and *shb1-D pif4* behaved like *pif4* (Figure 9B). Under blue light, *shb1-D* enhanced the expression of only *CHS* and *pif4* reduced the expression of both *CAB3* and *CHS*. The *shb1-D pif4* double mutant behaved like *shb1-D* under blue light, and the effects of *shb1-D* on the expression of these two genes were independent of *pif4* (Figure 9B). Therefore, PIF4 may specifically mediate SHB1 regulation on hypocotyl elongation and light-induced gene expression under red light, consistent with the specific effect of *shb1-D* on the expression of *PIF4* under red light but not blue light (Figures 8A and 9A).

***shb1-D* Promotes phyA Degradation under Far-Red Light**

To explore how the overexpression of SHB1 expands its signaling activity to far-red light, we examined the phyA protein level in dark-grown Ws and *shb1-D* seedlings after exposure to far-red light for several hours. The experiments also included MG132, a proteasome inhibitor, because phyA can be ubiquitinated by COP1 and undergoes proteasome-mediated degradation (Seo et al., 2004). A normal degradation pattern of phyA was observed in Ws after far-red light treatment, and a noticeable reduction in phyA protein level was observed 6 h after far-red light illumination (Figure 9C). phyA degradation was promoted in *shb1-D*, and an apparent reduction in phyA protein level was observed 3 h earlier
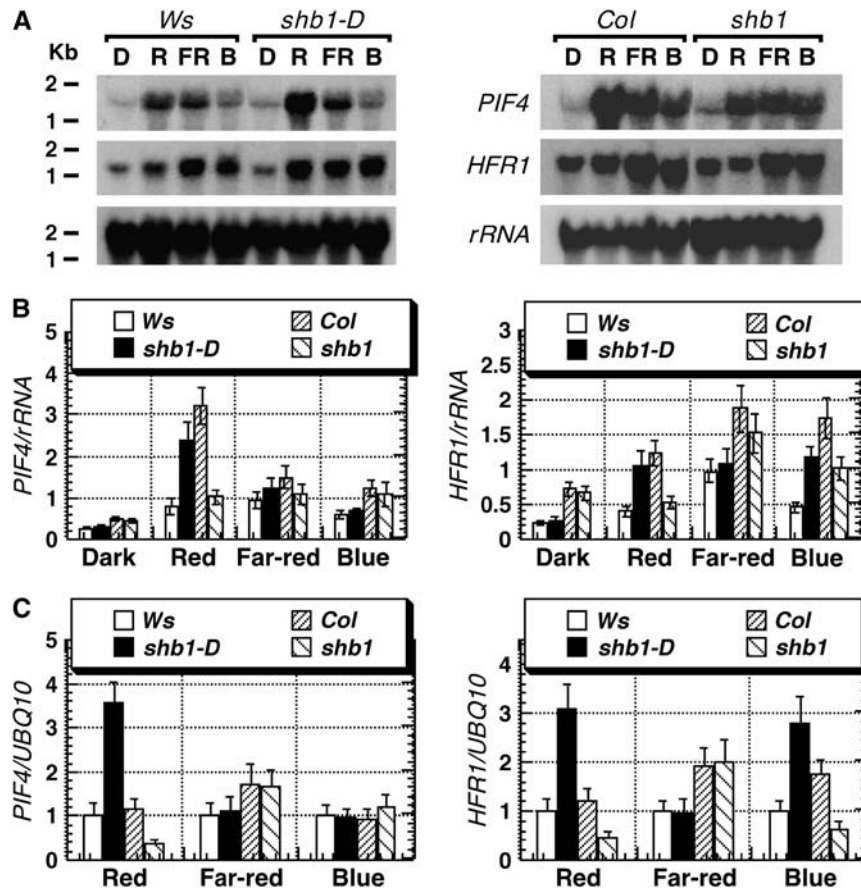
Figure 8. Mutations in *SHB1* Affect the Expression of *PIF4* and *HFR1*.

(A) RNA gel blot hybridization analysis of *PIF4* and *HFR1* in *shb1-D* and *shb1*. Total RNA was isolated from 5-d-old dark-grown Ws, *shb1-D*, Col, and *shb1* seedlings that received no light treatment (D) or were treated for 4 h with red (R), far-red (FR), or blue (B) light under the intensities specified for Figure 1A. The gel images for *PIF4* and *HFR1* expression in Col and *shb1* were overexposed to clearly show the decreases in the expression of the two genes.

(B) Normalization of *PIF4* and *HFR1* mRNA levels to 18 *rRNA* signals. The hybridization signals were detected with a PhosphorImager and quantified using the ImageQuant program. Data are presented as means ± SE from two independent experiments.
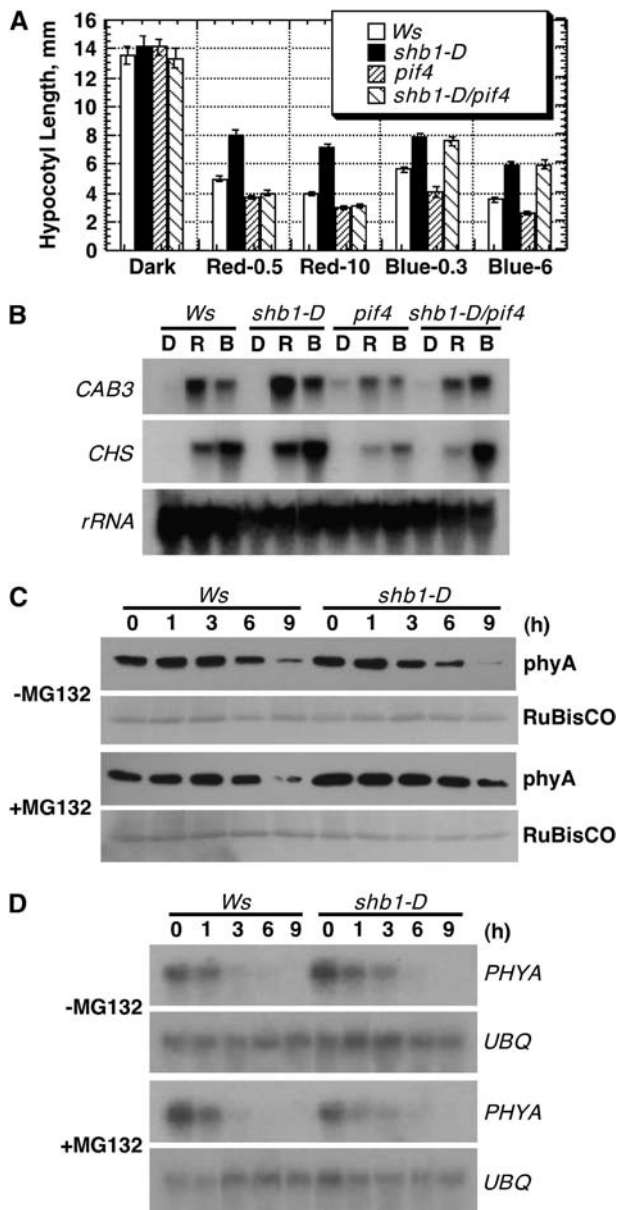
(C) Real-time PCR analysis of *PIF4* (left) or *HFR1* (right) expression in Ws, *shb1-D*, Col, and *shb1* under red, far-red, or blue light at the intensities specified for Figure 1A. PCR was performed on RT reaction using SYBR green PCR master mix and the 7500 Real Time PCR system. The levels of *PIF4* or *HFR1* expression were normalized to *UBQ10*. Data are presented as means ± SE from two independent experiments.

after far-red light treatment. Addition of MG132 partially attenuated the rate of phyA disappearance in the Ws wild type and also restored the rate of phyA degradation in *shb1-D* to a level comparable to that in the wild type under similar conditions (Figure 9C) (Seo et al., 2004). By contrast, *shb1-D* did not alter the decrease in *PHYA* transcription under far-red light, and an even slightly higher level of *PHYA* mRNA was noticed after far-red light treatment in *shb1-D* compared with that in the Ws wild type (Figure 9D). MG132 did not affect the level of *PHYA* mRNA under far-red light in either the wild type or *shb1-D*.

SHB1 Blue Light Signaling Involves HFR1

shb1 affected the expression of *HFR1* under both red and blue light (Figure 8A). Indeed, *shb1* and *hfr1-201* shared several similar phenotypes under blue light, such as cotyledon expan-

sion and pigment accumulation (Figures 3 and 4) (Duek and Fankhauser, 2003). *shb1* and *hfr1-201* also had phenotypes opposite to each other, such as hypocotyl elongation and cotyledon opening, under blue light (Figures 2 and 10B) (Duek and Fankhauser, 2003). The *shb1 hfr1-201* double mutant showed a long-hypocotyl phenotype under blue light, similar to that of the *hfr1-201* single mutant. The smaller effects of either *shb1* or *hfr1-201* on the expression of *CAB3* or *CHS* did not reveal a clear epistasis (see Supplemental Figure 6 online). Therefore, we examined the *shb1 hfr1-201* double mutant for the cotyledon-opening response (Figure 10B). Under relatively weak blue light, *shb1* seedlings fully opened their cotyledons, whereas Col wide-type seedlings just partially opened their cotyledons (Figure 10B, top). Under similar conditions, the cotyledons of *hfr1-201* were fully closed and *shb1 hfr1-201* showed a phenotype similar to that of *hfr1-201*. Under higher

blue light intensity, both Col and *shb1* seedlings fully opened their cotyledons, whereas *hfr1-201* seedlings only partially opened theirs (Figure 10B, bottom). The *shb1 hfr1-201* double mutant behaved like *hfr1-201*, suggesting an epistasis of *hfr1-201* to *shb1* in their control of the cotyledon-opening responses.

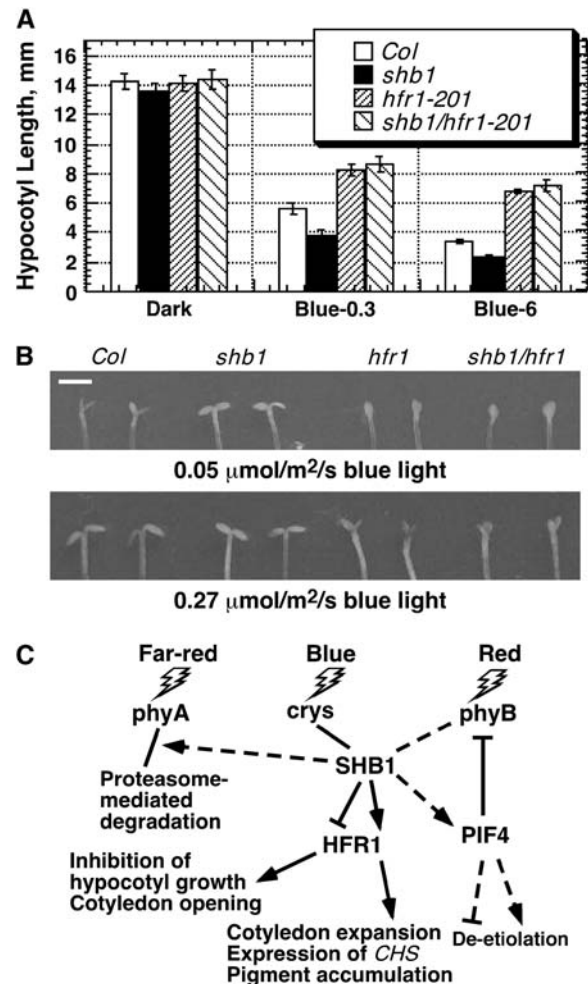**Figure 9.** SHB1 Acts Upstream of PIF4, and the *shb1-D* Mutation Promotes phyA Degradation.

(A) Hypocotyl growth responses of Ws, *shb1-D*, *pif4*, and *shb1-D pif4* seedlings to 0.5 or 10 μmol·m^{-2}·s^{-1} red light (Red-0.5 or Red-10) or 0.3 or 6 μmol·m^{-2}·s^{-1} blue light (Blue-0.3 or Blue-6) for 4 d. Data are presented as means $\pm$ SE.

(B) RNA gel blot analysis of *CAB3* and *CHS* expression on total RNA isolated from 5-d-old dark-grown Ws, *shb1-D*, *pif4*, and *shb1-D pif4* seedlings that received no light treatment (D) or were treated for 3 h with red (R) or blue (B) light under the intensities specified for Figure 1A.

(C) PhyA degradation in 5-d-old Ws and *shb1-D* seedlings that were treated with or without MG132 under far-red light (0.2 μmol·m^{-2}·s^{-1}) for the times indicated. RuBisCO, ribulose-1,5-bis-phosphate carboxylase/oxygenase.

(D) RNA gel blot hybridization analysis of *PHYA* and *UBQ10* mRNA levels in 5-d-old Ws and *shb1-D* seedlings that were treated with or without MG132 under far-red light (0.2 μmol·m^{-2}·s^{-1}) for the times indicated.

Figure 10. SHB1 Acts Upstream of HFR1, and the Roles of SHB1 in Light Signaling.

(A) Hypocotyl growth responses of Col, *shb1*, *hfr1-201*, and *shb1 hfr1-201* seedlings to 0.3 or 6 μmol·m^{-2}·s^{-1} blue light (Blue-0.3 or Blue-6) for 4 d. Data are presented as means $\pm$ SE.

(B) Cotyledon-opening responses of 4-d-old Col, *shb1*, *hfr1-201*, and *shb1 hfr1-201* seedlings to weak blue light (0.05 μmol·m^{-2}·s^{-1}) or moderate blue light (0.27 μmol·m^{-2}·s^{-1}). Bar = 1.5 mm.

(C) SHB1 acts in cry- and possibly phy-mediated light signaling pathways and regulates various light responses either positively (arrows) or negatively (T-bars). SHB1 signaling may involve HFR1 in the control of hypocotyl elongation, cotyledon opening and expansion, expression of *CHS*, and pigment accumulation (solid lines). Overexpression of *SHB1* activates PIF4-mediated red light signaling and also promotes the proteasome-mediated degradation of phyA and hypocotyl elongation under far-red light (dotted lines).

DISCUSSION

We have identified two *SHB1* mutant alleles, an overexpression allele, *shb1-D*, and a knockout allele, *shb1*. The phenotypes of *shb1-D* and *shb1* are opposing each other in most cases and together suggest the different roles of SHB1 in controlling various light responses. For example, lack of *SHB1* expression in *shb1* resulted in a short hypocotyl, smaller cotyledons, accelerated cotyledon opening, reduced expression of *CHS*, and reduced accumulation of anthocyanins under blue light (Figures 2 to 4). By contrast, overexpression of *SHB1* in *shb1-D* led to a longer hypocotyl under red, far-red, and blue light, an enhanced far-red light preconditioned block of greening response, larger cotyledons under red and blue light, enhanced expression of *CAB3* and *CHS*, and enhanced accumulation of pigments (Figures 1, 3, and 4). Loss of *SHB1* expression in *shb1* also created a long-petiole phenotype under white light, whereas overexpression of *SHB1* in *shb1-D* led to shorter petioles and smaller leaves under white light (Figure 3). Therefore, we propose a model in which SHB1 negatively regulates the inhibition of hypocotyl elongation, cotyledon opening, and leaf expansion but positively regulates cotyledon expansion, the inhibition of petiole elongation, the expression of *CHS*, and pigment accumulation (Figure 10C). Considering that all of the photoreceptors seem to interact in numerous responses, we still could not rule out a role of SHB1 in phototropin-mediated blue light signaling.

shb1 showed photomorphogenic phenotypes primarily under blue light, although reduced accumulation of anthocyanins and expression of *CHS* were also observed in *shb1* under far-red light (Figure 4). By contrast, overexpression of *SHB1* in *shb1-D* created various photomorphogenic phenotypes under red, far-red, and blue light (Figures 1, 3, and 4). A similar case has been observed for phyA. Mutation in *PHYA* led to a long hypocotyl only under far-red light, but overexpression of *PHYA* in *Arabidopsis* and other dicots created a short-hypocotyl phenotype under red, far-red, and white light (Boylan and Quail, 1991; Nagatani et al., 1991). Interestingly, overproduction of HFR1:GFP also caused a hypersensitive hypocotyl growth response to red light (Yang et al., 2005), although *hfr1* exhibited a hyposensitive hypocotyl growth response only to far-red and blue light (Soh et al., 2000; Duek and Fankhauser, 2003; Huq and Quail, 2005). However, these cases may not sufficiently explain the phenotypes of *shb1-D* under all light wavelengths tested.

Considering the extremely low abundance of *SHB1* transcript, the level of SHB1 protein may be limiting for red and far-red light signaling. Alternatively, the lack of hypocotyl or cotyledon phenotype in *shb1* under red or far-red light may be attributable to a redundant function of SHB1 homologues. Overexpression of *SHB1* enhances the expression of *PIF4* under red light, and *pif4* is epistatic to *shb1-D* in the red light–mediated hypocotyl elongation response (Figures 8, 9, and 10C). Overexpression of *SHB1* also promotes phyA protein degradation and hypocotyl elongation under far-red light (Figures 1, 9, and 10C). Under blue light, *shb1* suppressed the expression of *HFR1*, and *shb1* indeed showed several deetiolation phenotypes similar to those of *hfr1-201*, such as smaller cotyledons, reduced expression of *CHS*, and reduced accumulation of anthocyanins (Figures 3 and 4). Therefore, SHB1 and HFR1 have overlapping functions in reg-

ulating the blue light–mediated responses. However, the hypocotyl elongation and cotyledon-opening phenotypes of *shb1* were opposite to those of *hfr1-201* under blue light. Although the altered expression of *HFR1* in *shb1* does not explain its hypocotyl phenotype, genetic analysis indicates that HFR1 acts downstream of SHB1 (Figure 10).

On the other hand, *shb1-D* enhanced the expression of *HFR1* under blue light and resulted in several deetiolation phenotypes opposite to that of *hfr1-201*, such as cotyledon size, *CHS* expression, and pigment accumulation (Figures 3 and 4). As shown recently, overexpression of full-length *HFR1* or *HFR1:GFP* led to hypersensitive phenotypes opposite to that of *hfr1-201* under red, far-red, or blue light (Jang et al., 2005; Yang et al., 2005). The responses include hypocotyl and cotyledon growth and *CAB3* expression. Thus, several deetiolation phenotypes, but not the hypocotyl phenotype, of *shb1-D* can be explained well by the increased expression of *HFR1* in *shb1-D*. By contrast, SHB1 may either regulate hypocotyl elongation and cotyledon-opening responses through an HFR1-independent branch or act negatively upstream of HFR1.

Genetic analysis revealed a *phy*- or *cry*-like phenotype in *shb1-D phy* or *shb1-D cry* double mutants (Figures 5 and 6). However, epistatic interactions may not be revealed clearly because *shb1-D* is a dominant and gain-of-function allele. *phyA* and *phyB* have the most severe hypocotyl phenotypes under far-red or red light and *phyA* is almost blind to far-red light, whereas *shb1-D* has a moderate hypocotyl phenotype under these light conditions. Introduction of *shb1-D* into the *phyA* or *phyB* background did not enhance or suppress the severe hypocotyl phenotypes of *phyA* or *phyB*. Again, our data may not reveal much genetic interaction because in most cases the phenotype of the stronger mutation is always observed in these double mutants. In addition, the two single mutations cause a similar phenotype, and one may still observe the phenotype of the stronger mutation even if there is no genetic interaction. Under blue light, *cry1* has the most severe hypocotyl phenotype, and the situation observed for *shb1-D cry1* is similar to that for *shb1-D phyA* or *shb1-D phyB*. The hypocotyl phenotype of *shb1-D* is moderate and similar to that of *phyA* or *cry2* under blue light, and the response of *shb1-D phyA-211* or *shb1-D cry2* to blue light was indistinguishable from that of either of their parents. By contrast, *shb1* has an opposite hypocotyl phenotype to either *cry1* or *cry2*, and the *shb1 cry1* or *shb1 cry2* double mutant showed the *cry1* or *cry2* hypocotyl phenotype. Thus, expression of the *shb1* hypocotyl phenotype requires blue light, and such an epistasis reflects a dependence of the phenotype conferred by *shb1* on functional cryptochromes.

SHB1 contains an N-terminal SPX domain and a C-terminal EXS domain found in SYG1-like and XPR1-like proteins (Figure 7A; see Supplemental Figure 3 online). The human and mouse *XPR1* encodes a cell surface receptor for xenotropic and polytropic murine leukemia viruses, conferring susceptibility to infection with murine leukemia viruses (Tailor et al., 1999; Yang et al., 1999). PHO81 has been shown to serve as a putative sensor of phosphate level in yeast and presumably *Arabidopsis* (Hamburger et al., 2002; Neef and Kladde, 2003). A truncated version of yeast SYG1, containing the N-terminal SPX domain, has been shown to rescue the lethal phenotype of a mutation in the G-protein α-subunit (Spain et al., 1995). The truncated

protein does so by interacting directly with the G-protein β-subunit, and the interaction may inhibit the transduction of the mating pheromone signals. Apparently, a major function of the SPX domain in SYG1 is to mediate protein–protein interactions.

The EXS domain is also found in the yeast ERD1 protein (Hardwick et al., 1990). The region of EXS similarity contains several predicted transmembrane helices, suggesting a possible membrane localization of the proteins (Spain et al., 1995; Tailor et al., 1999; Yang et al., 1999). For example, three membrane-spanning motifs out of eight in yeast SYG1 reside in this region. Indeed, SYG1 was enriched in a plasma membrane fraction (Spain et al., 1995). Examination of the SHB1 protein sequence with PSORT also identified six weakly predicted integral membrane motifs. However, SHB1 is localized in the nucleus and the cytoplasm, like two other light signaling proteins, FHY1 and SRR1 (Figure 7B) (Huq and Quail, 2005; Ni, 2005). Thus, the EXS domain in SHB1 may have a distinct function from those in SYG1-like proteins. In summary, SHB1-like proteins exist in a variety of organisms, including yeast, fission yeast, *Neurospora*, worm, fly, mouse, and human. Although the function of most SHB1-like proteins remains to be determined in other organisms, we demonstrated the involvement of one member, SHB1, in regulating blue light responses specifically and/or possibly red and far-red light responses in *Arabidopsis*.

METHODS

Plant Growth Conditions, Genetic Screen, and Phenotypic Analysis

The *Arabidopsis thaliana shb1-D* mutant allele was isolated from a T-DNA insertion population in the Ws background (ABRC), and the *shb1* mutant allele was isolated from a SALK T-DNA insertion population in the Col background. Monochromatic red, far-red, or blue light was generated with LED SNAP-LITE (Quantum Devices). Light intensity and peak wavelength were measured with a SPEC-UV/PAR spectroradiometer (Apogee Instruments). For most light experiments, *Arabidopsis* seeds were surface-sterilized, plated on regular agar growth medium minus sucrose, stratified at 4°C for 3 d, treated with fluorescent white light for 0.5 to 1 h, and allowed to germinate and grow under monochromatic light for 4 d. Hypocotyl, cotyledon, and leaf images were taken using an Olympus digital Camedia C-700, and length and area were measured using ImageJ. Each measurement includes 40 to 50 seedlings. Petiole length and leaf area were measured for the first fully expanded true leaf. The chlorophyll and anthocyanin contents were measured as described (Kim et al., 2003).

Molecular Cloning and Characterization of *SHB1*

Plant genomic DNA was isolated using the DNeasy plant mini kit (Qiagen). Plant DNA sequences flanking the T-DNA right or left border in *shb1-D* were obtained using a pair of right border primers, XR2 and nested XR3, and a pair of left border primers, JL202 and nested JL270 (University of Wisconsin Knockout Facility), along with the adapter primers, AP1 and nested AP2, from a GenomeWalker kit (Clontech). The T-DNA insertion also caused a 32-bp deletion of the plant genomic sequence surrounding the insertion site. The phylogenetic analysis on SHB1 and its homologues was conducted using the ClustalX 1.83 software program (http://bips.u-strasbg.fr/fr/Documentation/ClustalX/). Multiple alignment mode and protein weight matrix Gonnet series with gap opening set 20 were chosen for the analysis. The phylogenetic tree was constructed using Bootstrap

N-J tree mode with bootstrap trial number 1000 and was viewed using the TreeView software program (taxonomy.zoology.gla.ac.uk/rod/treeview. html). The presence or absence of integral membrane motifs was predicted using PSORT (http://psort.nibb.ac.jp).

Total RNA was isolated from plant tissues using the SV total RNA isolation system (Promega). Ten micrograms of total RNA was loaded on each lane for RNA gel blot analysis as described (Kang et al., 2005). Total RNA was used to perform the RT reaction using SuperScript RNase H⁻ reverse transcriptase and gene-specific primers (Invitrogen). PCR was subsequently performed on 0.5 to 1 μL of RT reaction using Taq polymerase. Real-time PCR was performed on RT reaction using SYBR green PCR master mix and the 7500 Real Time PCR system (Applied Biosystems). Each experiment was repeated twice with completely independent biological samples, and three RT-PCR reactions were performed for each of the samples. Gene expression data were presented relative to average values for the Ws wild type using a relative quantification assay, after normalization to the control *UBQ10* (Applied Biosystems).

To examine phyA protein or *PHYA* mRNA level in Ws or *shb1-D*, 5-d-old seedlings grown in darkness were treated with far-red light (0.2 μmol·m⁻²·s⁻¹) for various times on regular agar growth medium. For experiments involving MG132, 5-d-old dark-grown seedlings were collected from regular agar growth medium and incubated in liquid growth medium containing either 50 μM MG132 (dissolved in DMSO) or DMSO in an equivalent volume added to the liquid growth medium under far-red light for the indicated times (Seo et al., 2004; Jang et al., 2005). Total plant proteins were prepared from seedlings, and phyA was detected by protein gel blot analysis using phyA-specific monoclonal antibodies as described previously (Ni et al., 1998).

Overexpression of *SHB1* and Complementation of *shb1*

For overexpression analysis, *SHB1* cDNA was amplified from the CD4-22 cDNA library (ABRC) with end-incorporated *Nhe*I and *Xma*I restriction sites and cloned into a modified PBI121 vector, in which the *GUS* gene was replaced with a *GFP* gene. A *Hind*III-*Eco*RI fragment from the modified PBI121 vector, containing CaMV 35S promoter, *SHB1* and *GFP* coding sequences, and 3′ terminator, was then subcloned into pCAMBIA3300 vector. For phenotypic complementation, a 4.7-kb genomic fragment, spanning 1.2 kb upstream to 0.5 kb downstream of the *SHB1* coding sequence, was generated using PCR from BAC clone T30C3 (ABRC) and contained end-incorporated *Xma*I and *Pst*I restriction sites. The PCR fragment was then cloned into binary vector pCAMBIA3300.

Subcellular Localization Studies

For transient expression assay, *SHB1* cDNA was amplified from the CD4-22 cDNA library (ABRC) with end-incorporated *Nhe*I and *Xma*I restriction sites and cloned into PBI221 vector. The resulting vector carries a *SHB1*:*GUS* fusion under the control of the CaMV 35S promoter. Transformation of *SHB1*:*GUS* into onion (*Allium cepa*) epidermal cells and 4′,6-diamidino-2-phenylindole staining were performed as described previously (Ni et al., 1998). The transfected onion epidermal peels were incubated in darkness for 24 h and then either received no light treatment or were treated with white, red, far-red, or blue light for 4 or 8 h. GUS staining was performed and nuclear images were acquired using a Nikon Eclipse E800 microscope with a Cool Cam color CCD camera (Cool Camera) and Imago Pro Plus version 3.0 software (Media Cybermetics).

Double Mutant Analysis

phyA-211 (Col), *phyB-9* (Col), and *cry2-1* (Col) mutants were obtained from the Arabidopsis Stock Center, and *cry1-304* (Col) was kindly provided by Chentao Lin. *phyB-9* is an ethyl methanesulfonate mutant,

whereas *phyA-211*, *cry1-304*, and *cry2-1* contain large deletions. Homozygous *phyA-211* or *phyB-9* was selected at the F2 generation based on a striking long-hypocotyl phenotype under far-red or red light, respectively. Homozygous *cry1* or *cry2* was selected at the F2 generation based on a long-hypocotyl phenotype under blue light but verified by PCR genotyping at F3. Both *shb1-D* (Ws) and *shb1* (Col) contain a T-DNA insertion near or in their coding regions. Homozygous *shb1-D* or *shb1* was selected by a linked resistance to kanamycin from the F3 individuals in a homozygous *phyA-211*, *phyB-9*, *cry1*, or *cry2* background. An extra step was taken to generate *shb1-D cry1* and *shb1 cry1* double mutants, because the mutations are both on chromosome 4 but are 37 centimorgans apart. Recombinants were selected based on their long-hypocotyl phenotype under blue light and their resistance to kanamycin. Ws × Col wild type was also generated to control the difference in hypocotyl growth between crosses of different ecotypes.

The *shb1-D pif4* double mutant was generated by genetic cross, and both *shb1-D* and *pif4* are in the Ws background and contain a T-DNA insertion and linked resistance to kanamycin near or in their coding regions (Huq and Quail, 2002). Homozygous *shb1-D* or *pif4* was genotyped using PCR at F2 or F3. *hfr1-201* was kindly provided by Pill-Soon Song and was used to generate the *shb1 hfr1-201* double mutant. Both *shb1* and *hfr1-201* are in the Col background and contain a T-DNA insertion and linked resistance to kanamycin near or in their coding regions (Soh et al., 2000). Homozygous *shb1* or *hfr1-201* was also genotyped using PCR at F2 or F3.

Accession Numbers

Sequence data from this article can be found in the GenBank/EMBL data libraries under accession numbers *At4g25350* (*SHB1*), *At2g43010* (*PIF4*), and *At1g02340* (*HFR1*).

Supplemental Data

The following materials are available in the online version of this article.

Supplemental Figure 1. Verification of the T-DNA Insertions in *shb1-D* and *shb1* with PCR.

Supplemental Figure 2. Double Mutant Analysis of *shb1-D* with *phyA-211* and *cry* Mutants under Blue Light.

Supplemental Figure 3. Phylogenetic Analysis of SHB1 with Its Homologues.

Supplemental Figure 4. Alignment of SHB1 with Its Homologues Used for the Phylogenetic Analysis.

Supplemental Figure 5. Sequence Alignment of SHB1 with Yeast SYG1.

Supplemental Figure 6. RNA Gel Blot Analysis of *CAB3* and *CHS* Expression in the *shb1 hfr1-201* Double Mutant.

ACKNOWLEDGMENTS

REFERENCES

Ahmad, M., Jarrilo, J.A., Smirnova, O., and Cashmore, A.R. (1998). The cry1 blue light photoreceptor of *Arabidopsis* interacts with phytochrome A *in vitro.* Mol. Cell **1,** 939–948.

Bouly, J.P., Giovani, B., Djamei, A., Mueller, M., Zeugner, A., Dudkin, E.A., Batschauer, A., and Ahmad, M. (2003). Novel ATP-binding and autophosphorylation activity associated with *Arabidopsis* and human cryptochrome-1. Eur. J. Biochem. **270,** 2921–2928.

Boylan, M.T., and Quail, P.H. (1991). Phytochrome A overexpression inhibits hypocotyl elongation in transgenic Arabidopsis. Proc. Natl. Acad. Sci. USA **88,** 10806–10810.

Cashmore, A.R. (2003). Cryptochromes: Enabling plants and animals to determine circadian time. Cell **114,** 537–543.

Choi, G., Yi, H., Lee, J., Kwon, Y.K., Soh, M.S., Shin, B., Luka, Z., Hahn, T.R., and Song, P.S. (1999). Phytochrome signalling is mediated through nucleoside diphosphate kinase 2. Nature **401,** 610–613.

Colón-Carmona, A., Chen, D.L., Yeh, K.-C., and Abel, S. (2000). Aux/IAA proteins are phosphorylated by phytochrome in vitro. Plant Physiol. **124,** 1728–1738.

Duek, P.D., and Fankhauser, C. (2003). HFR1, a putative bHLH transcription factor, mediates both phytochrome A and cryptochrome signaling. Plant J. **34,** 827–836.

Fankhauser, C., Yeh, A.C., Lagarias, J.C., Zhang, H., Elich, T.D., and Chory, J. (1999). PKS1, a substrate phosphorylated by phytochrome that modulates light signaling in *Arabidopsis.* Science **284,** 1539–1541.

Guo, H., Duong, H., Ma, N., and Lin, C. (1999). The *Arabidopsis* blue light receptor cryptochrome 2 is a nuclear protein regulated by a blue light-dependent post-translational mechanism. Plant J. **19,** 279–287.

Guo, H., Mockler, T., Duong, H., and Lin, C. (2001). SUB1, an *Arabidopsis* Ca^{2+}-binding protein involved in cryptochrome and phytochrome coaction. Science **291,** 487–490.

Guo, H., Yang, H., Mockler, T., and Lin, C. (1998). Regulation of flowering time by *Arabidopsis* photoreceptors. Science **279,** 1360–1363.

Hamburger, D., Rezzonico, E., MacDonald-Comber Petetot, J., Somerville, C., and Poirier, Y. (2002). Identification and characterization of the Arabidopsis *PHO1* gene involved in phosphate loading to the xylem. Plant Cell **14,** 889–902.

Hardwick, K.G., Lewis, M.J., Semenza, J., Dean, N., and Pelham, H.R. (1990). ERD1, a yeast gene required for the receptor-mediated retrieval of luminal ER proteins from the secretory pathway. EMBO J. **9,** 623–630.

Huq, E., and Quail, P.H. (2002). PIF4, a phytochrome-interacting bHLH factor, functions as a negative regulator of phytochrome B signaling in *Arabidopsis.* EMBO J. **21,** 2441–2450.

Huq, E., and Quail, P.H. (2005). Phytochrome signaling. In Handbook of Photosensory Receptors, W.R. Briggs and J.L. Spudich, eds (Weinheim, Germany: Wiley VCH), pp. 151–170.

Jang, I.C., Yang, J.Y., Seo, H.S., and Chua, N.H. (2005). HFR1 is targeted by COP1 E3 ligase for post-translational proteolysis during phytochrome A signaling. Genes Dev. **19,** 593–602.

Jones, A.M., Ecker, J.R., and Chen, J.G. (2003). A reevaluation of the role of the heterotrimeric G protein in coupling light responses in *Arabidopsis.* Plant Physiol. **131,** 1623–1627.

Kang, X., Chong, J., and Ni, M. (2005). HYPERSENSITIVE TO RED AND BLUE 1, a ZZ-type zinc finger protein, regulates phytochrome B-mediated red and cryptochrome-mediated blue light responses. Plant Cell **17,** 822–835.

Kim, D.H., Kang, J.G., Yanga, S.S., Chung, K.S., Song, P.S., and Park, C.M. (2002). A phytochrome-associated protein phosphatase 2A modulates light signals in flowering time control in Arabidopsis. Plant Cell **14,** 3043–3056.

Kim, J., Yi, H., Choi, G., Shin, B., Song, P.S., and Choi, G. (2003). Functional characterization of phytochrome interacting factor 3 in phytochrome-mediated light signal transduction. Plant Cell **15,** 2399–2407.

Kircher, S., Kozma-Bognar, L., Kim, L., Adam, E., Harter, K., Schafer, E., and Nagy, F. (1999). Light quality-dependent nuclear import of the plant photoreceptors phytochrome A and B. Plant Cell **11,** 1445–1456.

Kleiner, O., Kircher, S., Harter, K., and Batschauer, A. (1999). Nuclear localization of the *Arabidopsis* blue light receptor cryptochrome 2. Plant J. **19,** 289–296.

Lin, C., Yang, H., Guo, H., Mockler, T., Chen, J., and Cashmore, A.R. (1998). Enhancement of blue-light sensitivity of *Arabidopsis* seedlings by a blue light receptor cryptochrome 2. Proc. Natl. Acad. Sci. USA **95,** 2686–2690.

Liu, X.L., Covington, M.F., Fankhauser, C., Chory, J., and Wagner, D.R. (2001). *ELF3* encodes a circadian clock-regulated nuclear protein that functions in an *Arabidopsis* PHYB signal transduction pathway. Plant Cell **13,** 1293–1304.

McCormack, A.C., and Terry, M.J. (2002). Light-signaling pathways leading to the coordinated expression of *HEMA1* and *Lhcb* during chloroplast development in *Arabidopsis thaliana.* Plant J. **32,** 549–559.

Møller, S.G., Kim, Y.S., Kunkel, T., and Chua, N.H. (2003). PP7 is a positive regulator of blue light signaling in Arabidopsis. Plant Cell **15,** 1111–1119.

Nagatani, A., Kay, S.A., Deak, M., Chua, N.H., and Furuya, M. (1991). Rice type I phytochrome regulates hypocotyl elongation in transgenic tobacco seedlings. Proc. Natl. Acad. Sci. USA **88,** 5207–5211.

Neef, D.W., and Kladde, M.P. (2003). Polyphosphate loss promotes SNF/SWI- and Gcn5-dependent mitotic induction of PHO5. Mol. Cell. Biol. **23,** 3788–3797.

Neff, M.M., Fankhauser, C., and Chory, J. (2000). Light: An indicator of time and place. Genes Dev. **14,** 257–271.

Neuhaus, G., Bowler, C., Hiratsuka, K., Yamagata, H., and Chua, N.H. (1997). Phytochrome-regulated repression of gene expression requires calcium and cGMP. EMBO J. **16,** 2554–2564.

Ni, M. (2005). Integration of light signaling with photoperiodic flowering and circadian regulation. Cell Res. **15,** 559–566.

Ni, M., Tepperman, J.M., and Quail, P.H. (1998). PIF3, a phytochrome-interacting factor necessary for normal photoinduced signal transduction, is a novel basic helix-loop-helix protein. Cell **95,** 657–667.

Ni, M., Tepperman, J.M., and Quail, P.H. (1999). Binding of phytochrome B to its nuclear signaling partner PIF3 is reversibly induced by light. Nature **400,** 781–784.

Okamoto, H., Matsui, M., and Deng, X.W. (2001). Overexpression of the heterotrimeric G-protein α-subunit enhances phytochrome-mediated inhibition of hypocotyl elongation in Arabidopsis. Plant Cell **13,** 1639–1651.

Osterlund, M.T., Hardtke, C.S., Wei, N., and Deng, X.W. (2000). Targeted destabilization of HY5 during light-regulated development of *Arabidopsis.* Nature **405,** 462–466.

Ryu, J.S., et al. (2005). Phytochrome-specific type 5 phosphatase controls light signal flux by enhancing phytochrome stability and affinity for a signal transducer. Cell **120,** 395–406.

Seo, H.S., Watanabe, E., Tokutomi, S., Nagatani, A., and Chua, N.H. (2004). Photoreceptor ubiquitination by COP1 E3 ligase desensitizes phytochrome A signaling. Genes Dev. **18,** 617–622.

Seo, H.S., Yang, J.Y., Ishikawa, M., Bolle, C., Ballesteros, M.L., and Chua, N.H. (2003). LAF1 ubiquitination by COP1 controls photomorphogenesis and is stimulated by SPA1. Nature **423,** 995–999.

Shalitin, D., Yang, H., Mockler, T.C., Maymon, M., Guo, H., Whitelam, G.C., and Lin, C. (2002). Regulation of *Arabidopsis* cryptochrome 2 by blue-light-dependent phosphorylation. Nature **417,** 763–767.

Shalitin, D., Yu, X., Maymon, M., Mockler, T., and Lin, C. (2003). Blue light–dependent in vivo and in vitro phosphorylation of Arabidopsis cryptochrome 1. Plant Cell **15,** 2421–2429.

Soh, M.S., Kim, Y.M., Han, S.J., and Song, P.S. (2000). REP1, a basic helix-loop-helix protein, is required for a branch pathway of phytochrome A signaling in *Arabidopsis.* Plant Cell **12,** 2061–2073.

Spain, B.H., Koo, D., Ramakrishnan, M., Dzudzor, B., and Colicelli, J. (1995). Truncated forms of a novel yeast protein suppress the lethality of a G protein α subunit deficiency by interacting with the β subunit. J. Biol. Chem. **270,** 25435–25444.

Staiger, D., Allenbach, L., Salathia, N., Fiechter, V., Davis, S.J., Millar, A.J., Chory, J., and Fankhauser, C. (2003). The *Arabidopsis SRR1* gene mediates phyB signaling and is required for normal circadian clock function. Genes Dev. **17,** 256–268.

Sweere, U., Eichenberg, K., Lohrmann, J., Mira-Rodado, V., Baurle, I., Kudla, J., Nagy, F., Schafer, E., and Harter, K. (2001). Interaction of the response regulator ARR4 with phytochrome B in modulating red light signaling. Science **294,** 1108–1111.

Tailor, C.S., Nouri, A., Lee, C.G., Kozak, C., and Kabat, D. (1999). Cloning and characterization of a cell surface receptor for xenotropic and polytropic murine leukemia viruses. Proc. Natl. Acad. Sci. USA **96,** 927–932.

Wang, H., Ma, L.G., Li, J.M., Zhao, H.Y., and Deng, X.W. (2001). Direct interaction of *Arabidopsis* cryptochromes with COP1 in light control development. Science **294,** 154–158.

Wang, Y., Ribot, C., Rezzonico, E., and Poirier, Y. (2004). Structure and expression profile of the Arabidopsis *PHO1* gene family indicates a broad role in inorganic phosphate homeostasis. Plant Physiol. **135,** 400–411.

Ward, J.M., Cufr, C.A., Denzel, M.A., and Neff, M.M. (2005). The Dof transcription factor OBP3 modulates phytochrome and cryptochrome signaling in *Arabidopsis.* Plant Cell **17,** 475–485.

Wykoff, D.D., and O'Shea, E.K. (2001). Phosphate transport and sensing in *Saccharomyces cerevisiae.* Genetics **159,** 1491–1499.

Yang, H., Tang, R., and Cashmore, A.R. (2001). The signaling mechanism of Arabidopsis CRY1 involves direct interaction with COP1. Plant Cell **13,** 2573–2587.

Yang, H., Wu, Y., Tang, R., Liu, D., Liu, Y., and Cashmore, A.R. (2000). The C-termini of *Arabidopsis* cryptochrome mediate a constitutive light response. Cell **103,** 815–827.

Yang, J., Lin, R., Sullivan, J., Hoecker, U., Liu, B., Xu, L., Deng, X.W., and Wang, H. (2005). Light regulates COP1-mediated degradation of HFR1, a transcription factor essential for light signaling in *Arabidopsis.* Plant Cell **17,** 804–821.

Yang, Y.L., Guo, L., Xu, S., Holland, C.A., Kitamura, T., Hunter, K., and Cunningham, J.M. (1999). Receptors for polytropic and xenotropic mouse leukaemia viruses encoded by a single gene at Rmc1. Nat. Genet. **21,** 216–219.

Yeh, K., and Lagarias, C. (1998). Eukaryotic phytochromes: Light-regulated serine/threonine protein kinases with histidine kinase ancestry. Proc. Natl. Acad. Sci. USA **95,** 13976–13981.